# Differential Epipolar Constraint in Mobile Robot Egomotion Estimation

Xavier Armangué†*         Helder Araújo‡         Joaquim Salvi†

†Institut de Informàtica i Aplicacions
Universitat de Girona
Av. Lluís Santaló, s/n, E-17071 Girona (Spain)
{armangue,qsalvi}@eia.udg.es

‡Instituto de Sistemas e Robótica
Universidade de Coimbra
Polo II, 3030 Coimbra (Portugal)
helder@isr.uc.pt

## Abstract

*The estimation of camera egomotion is a well established problem in computer vision. Many approaches have been proposed based on both the discrete and the differential epipolar constraint. The discrete case is mainly used in self-calibrated stereoscopic systems, whereas the differential case deals with an unique moving camera. This article surveys several methods for mobile robot egomotion estimation covering more than 0.5 million samples using synthetic data. Results from real data are also given. The surveyed algorithms have been programmed and are available on the Internet:*
http://eia.udg.es/~armangue/research.

## 1. Introduction

Considering the binocular case, that is two views from a stereoscopic system or two different views from an unique moving camera, an interesting relationship is defined in the so-called epipolar geometry [4]. The epipolar geometry is contained in the fundamental matrix which includes the intrinsic parameters of both cameras and the position and orientation of one camera with respect to the other. The fundamental matrix can be used to reduce the matching process among the viewpoints and to get the camera pose in active systems where optical and geometrical parameters might change dynamically depending on the imaged scene. Two main principles are used in egomotion estimation: a) the discrete epipolar constraint; and b) the differential epipolar geometry.

The discrete epipolar constraint was formulated by Longuet-Higgins [6]. In this case the relative 3D displacement between both views is recovered by the epipolar constraint from a set of correspondences in both image

planes [9]. In addition, the differential case is the infinitesimal version of the discrete case, in which both views are always obtained from an unique moving camera [5, 10]. Considering the camera velocity slow enough and a high imaging rate, the relative displacement between two consecutive images becomes small. Then, the 2D displacement of image points can be obtained from an image sequence leading to the estimation of the 3D camera motion.

This article is structured as follows. First, a brief state-of-art on egomotion estimation is presented. Section 3 deals with the adaptation from 6-DOF (Degrees Of Freedom) estimation to the 2-DOF common case of a mobile robot, by constraining the movement. Section 4 compares the results obtained by using synthetic and real images. The article ends with conclusions.

## 2. Comparative state-of-art

Methods based on the discrete epipolar constraint are set off from the essential matrix $\mathbf{E}$ (see equation (1)), where $q$ is the projection of a 3D object point on the image plane of the first camera expressed in metric coordinates, $q'$ is the projection of the same object point in the second camera, $^C\mathbf{R}_{C'}$ is the rotation matrix that relates the orientation of the second camera with respect to the first, and $^C\hat{t}_{C'}$ is the antisymmetric matrix of the translation vector $^Ct_{C'}$ expressing the origin of the second camera with respect to the first. Then, the discrete epipolar constraint is given by,

$$q^T\mathbf{E}q' = 0, \qquad \mathbf{E} = {}^C\mathbf{R}_{C'}{}^T{}^C\hat{t}_{C'} \tag{1}$$

whereas differential methods are set off from two matrices (see equations (2) and (3)). These matrices encode the information about the linear $v$ and angular $w$ velocity of the camera [3].

$$q^T\hat{v}\dot{q} + q^T s q = 0 \tag{2}$$

$$s = \frac{1}{2}\left(\hat{w}\hat{v} + \hat{v}\hat{w}\right) \tag{3}$$

**Table 1. Motion recovery methods**

| Discrete Case | Differential Case |
|---|---|
| *Linear techniques* | |
| Longuet-Higgins (1981) | Zhuang et al. (1988)[1] |
| Tsai, Huang (1984) | Heeger, Jepson (1992-93) |
| Toscani, Faugeras (1986) | Kanatani (1993)[1] |
| Tomasi, Kanade (1992) | Tomasi, Shi (1993-94) |
| | Brooks et al. (1998)[1] |
| | • Seven Points |
| | • Least Squares (LS) |
| | • Iteratatively Reweighted LS |
| | • Modified IRLS |
| | • Least Median Squares |
| | Ma et al. (1998-2000)[1] |
| | Baumela et al. (2000)[1] |
| *Nonlinear techniques* | |
| Horn (1990) | Prazdny (1980-81) |
| Weng et al. (1992) | Bruss, Horn (1983) |
| Taylor, Kriegman (1995) | Zhang, Tomasi (1999) |
| Soatto, Brockett (1997) | |
| Ma et al. (1998) | |

Approaches to motion estimation can be classified into discrete and differential methods depending on whether they use a set of point correspondences or optical flow. Moreover, they are classified into linear and nonlinear depending on the minimization technique used, see table 1. This article focuses on linear techniques based on the differential epipolar constraint and their adaptation to mobile robot movement as described in the next section.

## 3. Adaptation to mobile robotics

Due to the fact that the permitted movements of a robot moving on flat ground are limited, it is possible to impose geometrical constraints in the differential epipolar equation. Then, the number of potential solutions is reduced, enabling a considerable improvement of the results obtained. We have considered a mobile robot with 2-DOF, i.e. a forward translation and a rotation around itself. The robot coordinate system has been fixed so that the robot translates along $X_R$ and rotates around $Z_R$. These constraints force the following considerations:

- The camera placed on the robot cannot move freely, so that camera velocity ($v_c$ and $w_c$) and robot velocity ($v_r$ and $w_r$) are equivalent ($v_r = v_c$ and $w_r = w_c$).

- The motion with respect to the camera coordinate system depends on its position. The camera is placed at

---

[1] Method based on the Differential Epipolar Constraint.

height $h$ along $Z_R$ so that $X_C$ axis is parallel to $Y_R$ and orthogonal to $X_R$. Then, $\alpha$ is the angle between the $X_R$ and $Z_C$ axis.

In such a configuration, the matrix that relates the camera and robot coordinate systems is known and equal to,

$$^R\mathbf{R}_C = \mathbf{R}_Z(-\frac{\pi}{2})\,\mathbf{R}_X(-\frac{\pi}{2} - \alpha) \qquad (4)$$

$$^R t_C = (0,0,h)^T \qquad (5)$$

$$^C\mathbf{R}_R = \mathbf{R}_X(\frac{\pi}{2} + \alpha)\,\mathbf{R}_Z(\frac{\pi}{2}) \qquad (6)$$

$$^C t_R = (0, -h\cos\alpha, h\sin\alpha)^T \qquad (7)$$

Then, the velocities can be transformed to the camera coordinate system obtaining,

$$^C v_c = {^C\mathbf{R}_R}{^R v_c} - {^C\mathbf{R}_R}{^R w_c} \times {^C t_R} \qquad (8)$$

$$^C w_c = {^C\mathbf{R}_R}{^R w_c} \qquad (9)$$

and simplifying,

$$^C v_c = (0, v_{r_1}\sin\alpha, v_{r_1}\cos\alpha)^T \qquad (10)$$

$$^C w_c = (0, w_{r_3}\cos\alpha, -w_{r_3}\sin\alpha)^T \qquad (11)$$

The camera motion is independent of $h$ and depends only on three parameters: both unknowns $v_{r_1}$ (linear velocity along $X_R$ axis) and $w_{r_3}$ (angular velocity around $Z_R$ axis); and the known angle $\alpha$. As a result, the symmetric matrix s in equation (3) can be simplified yielding,

$$\mathbf{s} = \begin{pmatrix} 0 & 0 & 0 \\ 0 & w_{r_3}v_{r_1}\sin\alpha\cos\alpha & \frac{1}{2}w_{r_3}v_{r_1}(\cos^2\alpha - \sin^2\alpha) \\ 0 & \frac{1}{2}w_{r_3}v_{r_1}(\cos^2\alpha - \sin^2\alpha) & -w_{r_3}v_{r_1}\sin\alpha\cos\alpha \end{pmatrix} \qquad (12)$$

where $s_1 = s_2 = s_3 = 0$, $s_4 = \frac{1}{2}w_{r_3}v_{r_1}\sin(2\alpha)$, $s_5 = \frac{1}{2}w_{r_3}v_{r_1}\cos(2\alpha)$ and $s_6 = -s_4$.

Equations (2) and (12) have been used to estimate the 2-DOF movement of the mobile robot.

## 4. Experimental results

Almost all the surveyed methods using the differential epipolar constraint (listed in table 1) were programmed and tested in the same conditions in order to allow an extensive comparison. The movement constraints described in the previous section were applied to six of these methods: LS, IRLS, MIRLS, LMedS proposed by Brooks et al. [2], the method proposed by Ma et al. [7] and the method proposed by Baumela et al. [1]). Results shown in this article permit to compare 6-DOF movement estimation methods with their adaptation to 2-DOF movement estimation of a mobile robot.

Several tests were done using synthetic data, with the goal of comparing the robustness of the methods in the

600

presence of image noise. We have used of a methodology similar to the one proposed by Tian et al. [8] and Ma et al. [7]. Moreover, the camera movement is estimated from a cloud of 50 3D points located in front of the camera and distributed along all the image field of view ( we considered a field of view varying between 30° and 90°). Next, the optical flow of every point was computed. Once the optical flow of the 50 points is computed, gaussian noise is added to every velocity component with a standard deviation varying from 0.05 up to 0.5 pixels. With the aim of studying the robustness of every method in any potential camera movement, all the potential camera orientations and translations were considered in ranges of 22.5°. Ten movement estimations are carried out for every camera pose. A new parameter $\alpha$, corresponding to the angle between the optical axis of the camera and the ground plane has been considered. Tests were done for several values of $\alpha$. The values used in the tests were 0°, 15°, 30°, 45°, 60°, 75° and 90°. It has been observed that the movement estimation presents a slight error at $\alpha = 45°$, which was the worst case.

Hence, given an image field of view of 30°, 60° or 90°, a linear/angular coefficient of 1, 5 or 10 and gaussian noise of 0.05 up to 0.5 pixels, a total of 655,360 movement estimations were computed for each method analyzed. Each estimate was compared to the real movement. The error in the linear velocity estimates was considered the angle between the real movement vector $v$ and the estimate $v_{est}$. The angle is computed using the following equation,

$$error_{lineal} = \cos^{-1}(v \cdot v_{est}) \qquad (13)$$

The discrepancy between the rotation matrix of the real angular movement $R$ and the estimated rotation matrix $R_{est}$ (obtained from the vector of angular velocities $w_{est}$), is used to compute the angular velocity error. The difference rotation matrix is defined as $\Delta R = R^T R_{est}$. The matrix $\Delta R$ is defined by a rotation axis and an angle. The error in the measurement of that angle is computed by using the following equation,

$$error_{angular} = \cos^{-1}\left(\frac{Tr(\Delta R) - 1}{2}\right) \qquad (14)$$

where $Tr(\Delta R)$ is the trace of the matrix.

Figure 1 shows the the results obtained by the movement estimation methods for the case of a mobile robot with a field of view of 90°, a coefficient linear/angular velocity equal to unity and $\alpha = 45°$, which is the worst case considered.

The methods adapted to robot motion do not present an error in the linear velocity estimation, because the methods intrinsically fix its direction. Hence, the error in the translation estimate for every method shown in figure 1 is zero. Actually, this fact implies that the error presented in the es-
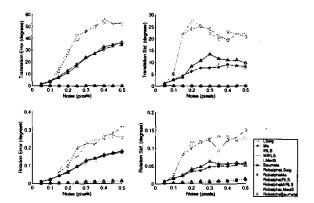


Figure 1. Results of general and simplified methods with synthetic images.
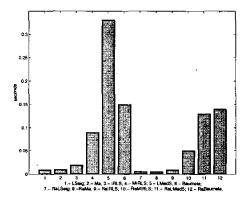


Figure 2. Computation time results for general and simplified methods with synthetic images.

timation of the angular velocity decreases considerably. Results on rotation estimation show that the adapted methods are more robust in the presence of image noise than their general versions (i.e. including all the 6-DOF). Figure 2 shows the computation times obtained by using MATLAB® and a PC Pentium III at 800 MHz, demonstrating that most of the methods give an estimation in less than 0.05 seconds, permitting their use in real-time applications.

The results obtained with real images are also quite accurate. Figure 3 compares the results given by LS and its adaptation to the mobile robot (RaLS), considering up to 80 test images where the camera has a tilt angle of -10° and the robot progresses and rotates with an angle of -0.1° in every two consecutive images. Figure 3 shows the accuracy on rotation and translation estimation and the vectors obtained. The error on translation estimation is zero in the
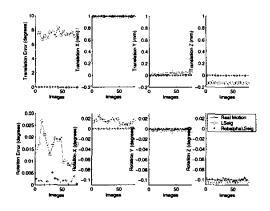
601

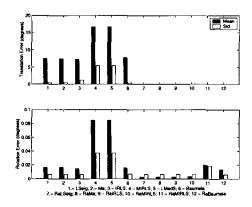**Figure 3. Example of motion estimation with real images.**



**Figure 4. Results of general and simplified methods with real images.**

adapted method while in the general method (6-DOF estimation) gives an error in the Z-axis since in that case it is difficult to distinguish between a camera rotation around Y-axis and a camera translation along X-axis. Finally, the rotation estimation is also more accurate using the adapted RaLS than the general method.

The same example described in the previous paragraph was tested for all the surveyed methods. The results obtained are represented in figure 4, which shows that the adapted 2-DOF methods are always more accurate than the general 6-DOF.

## 5. Conclusions

This article presents a new evaluation, comparison and classification of methods and techniques for egomotion estimation based on the differential epipolar constraint. The

article focuses on linear techniques based on the differential epipolar constraint. These techniques permit the estimation of the camera movement using optical flow without correspondences. The surveyed techniques were adapted in order to constrain the movement, considering the common situation of a 2-DOF mobile robot. Experimental results are given with synthetic data taking into account: gaussian noise, several camera fields of view, motion and camera position. The results obtained are more accurate and stable than their general versions, even under appreciable image noise. Results with real images show that the accuracy improves considerably as a result of considering a constrained movement.

Concluding, the 6-DOF movement estimation methods are quite sensitive to noise. Hence, these methods should be adapted constraining the number of DOF with the aim of reducing the error. In this article, the 2-DOF movement estimation of a mobile robot was evaluated and tested by using several methods of motion estimation.

## References

[1] L. Baumela, L. Agapito, P. Bustos, and I. Reid. Motion estimation using the differential epipolar equation. In *Proceedings of the 15th International Conference on Pattern Recognition*, volume 3, pages 848–851, Barcelona, 2000.

[2] M. J. Brooks, W. Chojnacki, A. Van Den Hengel, and L. Baumela. Robust techniques for the estimation of structure from motion in the uncalibrated case. In *Proceedings of the 5th Conference on Computer Vision*, volume 1, pages 281–295, Freiburg, Germany, June 1998.

[3] R. M. Haralick and L. G. Shapiro. *Computer and Robot Vision*, volume 2. Addison-Wesley Publishing Company, 1992.

[4] R. Hartley and A. Zisserman. *Multiple View Geometry in Computer Vision*. Cambridge University Press, 2000.

[5] K. Kanatani. Unbiased estimation and statistical analysis of 3-D rigid form two views. *IEEE Transactions on Pattern Analysis and Machine Intelligence*, 15(1):37–50, January 1993.

[6] H. C. Longuet-Higgins. A computer algorithm for reconstructing a scene from two projections. *Nature*, 293:133–135, 1981.

[7] Y. Ma, J. Košecká, and S. Sastry. Linera differential algorithm for motion recovery: A geometric approch. *International Journal of Computer Vision*, 36(1):71–89, 2000.

[8] T. Y. Tian, C. Tomasi, and D. J. Heeger. Comparison of approches to egomotion computation. In *Proceedings of the IEEE Conference on Computer Vision and Pattern Recognition*, pages 315–320, Los Alamitos, CA, USA, 1996.

[9] R. Y. Tsai and T. S. Huang. Uniqueness and estimation of three-dimensional motion parameters of rigid objects with curved surfaces. *IEEE Transactions on Pattern Analysis and Machine Intelligence*, 6(1):13–27, 1984.

[10] X. Zhuang, T. S. Huang, N. Ahuja, and R. M. Haralick. A simplified linear optic flow-motion algorithm. *Computer Vision, Graphics, and Image Processing*, 42:334–344, 1988.

602